Journal of Coastal Research	5	3	503-521	Charlottesville, Virginia	Summer 1989

Sediment Dynamics in the Lower Section of a Mixed Sand and Shell-Lagged Tidal Estuary, New Zealand

K. P. Black,† T. R. Healy‡ and M. G. Hunter*

†Victorian Institute of Marine Sciences
14 Parliament Place
Melbourne, Victoria 3002
Australia

‡Earth Sciences Department
University of Waikato
Hamilton, New Zealand

*Northland Harbour Board
Private Bag
Whangarei, New Zealand

ABSTRACT

BLACK, K. P.; HEALY, T. R., HUNTER, M. G., 1989. Sediment dynamics in the lower section of a mixed sand and shell-lagged tidal estuary, New Zealand. *Journal of Coastal Research*, 5 (3), 503-521. Charlottesville (Virginia), ISSN 0749-0208.

A series of field investigations and a numerical hydrodynamic model were applied to determine the sediment transport characteristics in the lower section of a large, tidally-dominated estuary at Whangarei Harbour, northeast New Zealand. The results show a consistent pattern in this unusual case where shell lag and shell/sand mixes have a dominant influence on the net sediment transport even though the estuary is subjected to a wide range of competent flows well above the sandy sediment threshold. A description of the estuary's sediment transport capacity, the influence of lagged beds, the relationship of morphology and sediments to tidal dynamics, especially tidal-cycle velocity residuals, and the implications for a proposed marine terminal in the study region are presented and discussed.

ADDITIONAL INDEX WORDS: *Sediment dynamics, tidal inlet, tidal deltas, numerical modelling, velocity residuals*

INTRODUCTION

Wangarei lies in the far north of the North Island of New Zealand near a developing *Pinus radiata* softwood industry requiring port facilities. When a site near the deep entrance to Wangarei Harbour was accepted as potentially the most suitable, the port authority, the Northland Harbour Board, initiated a series of estuarine investigations. The proposed port site is situated on a broad Holocene barrier spit which separates the harbour from the ocean, and the site is shared with New Zealand's sole oil refinery. To assess the proposed terminal's potential influence on the existing facilities and on the lower harbour in general, a detailed hydrodynamic and sediment dynamic investigation was established which then became the largest that had been undertaken in a New Zealand estuary. The field program was augmented by numerical hydrodynamic and sediment dynamic modelling (BLACK, 1983) and numerical and physical hydrodynamic modelling by the Danish Hydraulic Institute (DHI, 1982). The latter modelling is not discussed here but it assisted this study by providing background information and an additional framework to assess the descriptive models of sediment dynamics in the region.

Whangarei Harbour is one of several large meso-tidal estaurine lagoons on the northeast New Zealand coast. In the relatively unpolluted waters of this region, these estuaries support a prolific shell-fish population; cockles (*Chione stutchburyi*), dog cockles (*Dosinia subrosea* and *Glycymeris laticostata*), scallops (*Pecten nouvouzelandae*), pipis (*Paphies australe*), tuatua (*Paphies subtriangulatum*) and horse mussels (*Atrina zelandica*) are among the most common (BIO-RESEARCHES, 1976). Although sandy sediment is in ready supply along the coast (HEALY, 1981a), shell detritus is being constantly produced by the resident shellfish with the result that the bed in the estuary is characterized by locally-varying mixtures of sand and shell lag.

Concentrations of shell gravel lag were found to play an important stabilizing role in

88026 received 6 May 1988; accepted in revision 31 August 1988.
**Presently at: Beca-Carter, Hollings and Ferner, Consulting Engineers,P.O. Box 6345,Auckland, New Zealand*

determining the overall characteristics of the inlet stability and sediment dynamics. The shell was not only effective locally, but it also reduced sediment transport overall by limiting the availability of sand that could go into suspension in the strong flood and ebb-tidal currents. The interaction between bed type and flow dynamics is one of the primary considerations of this paper, which deals with the relationships between current flows, bed type and harbour morphology. The principles of estuarine sediment transport in such an inlet are concurrently examined.

SITE DESCRIPTION

Whangarei Harbour (Figure 1) is meso-tidal with a spring tidal prism of 186 x 10^6 m^3 (MILLAR, 1980). Currents reach 1.1-1.3 $m.s^{-1}$ in the entrance at spring tides. The lower harbour is a drowned river valley mostly contained by bedrock except for the spit at the south side which is composed of holocene sands (HEALY, 1981b).

Depths vary from about 30 m in the entrance throat to around 8 m in the Shoal Bay and the Main Shipping Channels. The two major shoals, Snake and McDonald Banks (Figure 1), represent the flood-tidal deltas relative to the entrance cross-section, and the Main Shipping Channel and Shoal Bay Channels around Snake Bank carry the bulk of the flow to the upper reaches (Figure 1). A striking feature of Snake Bank is its namesake; a snake-like ridge composed almost entirely of pipi shell detritus which weaves across its centre (Figure 2). Sand platforms are common around the fringes of the lower harbour from the entrance to One Tree Point and in McLeod Bay.

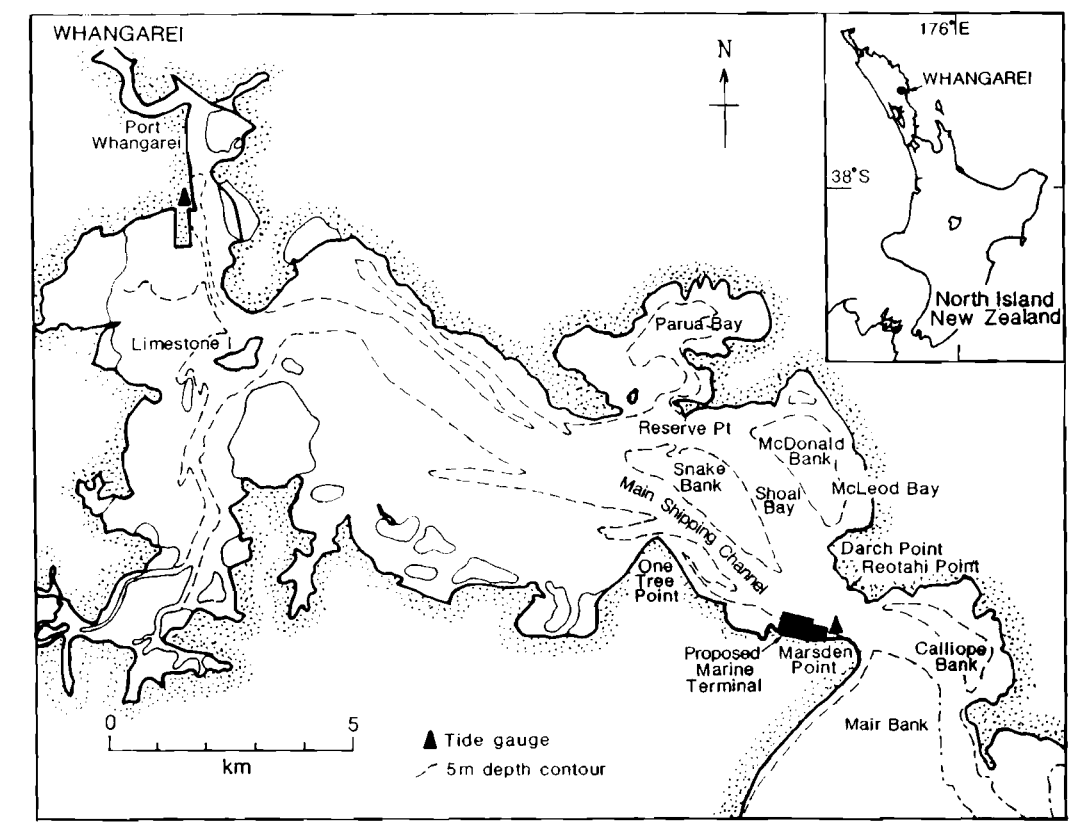

Figure 1. Whangarei Harbour on New Zealand's Northland coast.

Figure 2. (a) Oblique air photo of Snake Bank ebb shield. The sinuous shell ridges give rise to its name.

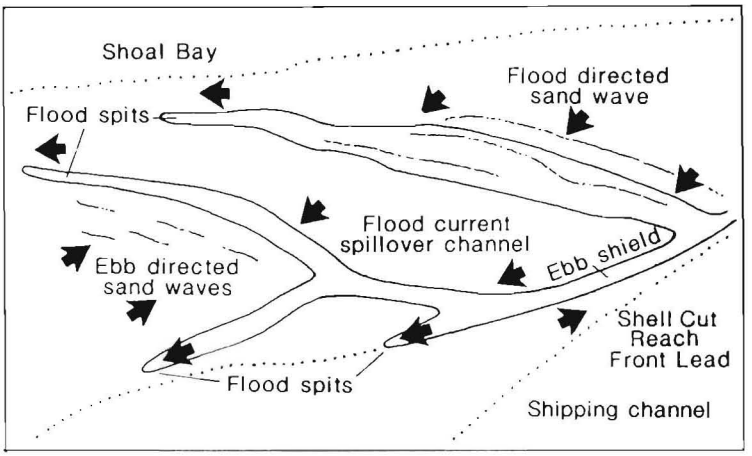

Figure 2. (b) The dominant sediment transport directions are inferred from the morpho-bathymetry, large-scale bedforms, and full tidal cycle velocity vector residuals (Black 1983).

EXPERIMENTAL TECHNIQUES

Many of the details of the field investigations at Whangarei are provided in HEALY *et al.* (1987) so that only a brief summary will be given here.

The nature of the sea bed was determined from a programme of diver observation, underwater photography and video, and bed sediment sampling (BLACK, *et al.*, 1981; BLACK, 1983). These results were then applied to interpret a side-scan sonar survey of the region (BLACK and HEALY, 1983).

The underwater video was operated from the Royal New Zealand Navy diving tender "Manawanui" which drifted or motored along the

channels with the camera suspended from the stern while the sea bed was observed and recorded on video film onboard. A lead weight was tied approximately 0.4 m below the camera to provide a scale, a measure of camera height above the bed and an indication of bottom compactness. Positions were fixed with Motorola Electronic Distance Measuring (EDM) equipment which was accurate to within +/− 1 m during static tests. Reference transponder stations were accurately placed by Northland Harbour Board surveyors.

The side-scan sonar survey was conducted with assistance from the Royal New Zealand Navy Hydrographic Branch over a 6 day period from 14-20 October, 1981. An E. G. & G. dual channel 100 kHz side-scan sonar was towed about 5 m above the sea bed. Decca EDM equipment was employed for horizontal position fixing.

During the study, the Royal New Zealand Navy Hydrographic Branch undertook a full hydrographic survey of the lower harbour and the ebb-tidal delta to provide accurate bathymetry for the proposed numerical and physical modelling and the overall field investigations.

Vertical current profiles were measured at a large number of sites at half to one hour intervals over full-tidal cycles for both neap and spring tides using a Braystoke BFM-010 multiparameter current meter. This meter simultaneously recorded speed, direction, temperature and salinity, while a built-in depth sounder provided accurate distances above the sea bed. Velocity was measured by counting impeller revolutions and a 100 s time interval was selected to average out shorter-period turbulent current fluctuations. The profile measurements were supplemented with drogue tracking (BLACK *et al.*, 1982; BLACK, 1983) and 4 Aanderaa RCM-4 current meters (DHI, 1982; BLACK, 1983) were each deployed for 2 months at 4 sites. In the tidally-dominated environment, the drogues were suspended some 1-2 m below the surface to allow them to pass over most shoaling areas and therefore the measured speeds will primarily reflect near-surface currents rather than those near the bed. Their paths were fixed using Motorola EDM equipment. Detailed measurements of sediment transport and sediment thresholds were made at several locations in the harbour and experimental procedures were described in BLACK and HEALY (1982, 1986).

NUMERICAL HYDRODYNAMIC MODELLING

As the lower harbour is well-mixed and 2-dimensional modelling was considered to be appropriate, simulations of tidal flows were made with the numerical hydrodynamic model (2DD) of Black (1983) which solves the 2-dimensional depth-averaged momentum and continuity equations for long waves,
where momentum is given by

$$\begin{aligned}
&\frac{\partial U}{\partial t} + \beta\left[\frac{U\partial U}{\partial x} + \frac{V\partial U}{\partial y}\right] - fV \\
&\quad = -\frac{g\partial\xi}{\partial x} - \frac{gU(U^2 + V^2)^{1/2}}{C^2(d + \xi)} \\
&\qquad + \frac{\rho_a\,\gamma\,|W|Wx}{\rho(d + \xi)} \\
&\qquad + A_H\left[\frac{\partial^2 U}{\partial x^2} + \frac{\partial^2 U}{\partial y^2}\right] \frac{\partial V}{\partial t} \qquad (1) \\
&\qquad + \beta\left[\frac{U\partial V}{\partial x} + \frac{V\partial V}{\partial y}\right] + fU \\
&\quad = -\frac{g\partial\xi}{\partial y} - \frac{gV(U^2 + V^2)^{1/2}}{C^2(d + \xi)} \\
&\qquad + \frac{\rho_a\,\gamma\,|W|Wx}{\rho(d + \xi)} \\
&\qquad + A_H\left[\frac{\partial^2 V}{\partial x^2} + \frac{\partial^2 V}{\partial y^2}\right]
\end{aligned}$$

and continuity is given by

$$\frac{\partial\xi}{\partial t} + \frac{\partial}{\partial x}(d + \xi)U + \frac{\partial}{\partial y}(d + \xi)\,V = 0 \qquad (2)$$

U, V are mean vertically- averaged velocities in the x, y directions respectively, g the gravitational acceleration, ξ the sea level above a horizontal datum, d the depth below datum, f the Coriolis parameter, ρ the water density, W the wind speed at 10 m above sea level, γ the wind resistance coefficient, ρ_a the density of air, C is Chezy's C, A_H is the horizontal eddy viscosity coefficient and β is a vertical integration correction factor (normally taken as 1).

2DD is semi-explicit and solves the hydrodynamic equations using a leap-frog, time-stepping procedure. The model includes a flooding and drying algorithm which was employed to

simulate the inundation and exposure of the inter-tidal sand banks. Depths were digitized on the cell walls (*e.g.* BLACK and GAY, 1987) rather than the more typical mid-point representation (LEENDERTSE, 1967). Twice as many depths are input which improves bathymetry resolution without increasing CPU requirements (BLACK, 1983). A 250 m-square grid of 24 by 23 cells was established for lower Whangarei Harbour and this resolved the important general flow features which are of interest in this paper.

Because of computer memory limitations, the up-harbour sea level boundary condition on the western model boundary was obtained from a 1-dimensional model simulation of the entire harbour (Figure 1). The explicit, 1-dimensional model, 1DD of BLACK (1983) includes all the terms in equation 1 with V set to zero. The eddy diffusion term was retained in the model without the derivative in y, and this has a standard physical interpretation if one assumes that the harbour flanks are free slipping. The 1-dimensional model included the longitudinal density gradients associated with the measured salinity changes from 34 ‰ at the entrance of 26 ‰ in the upper reaches (MILLAR, 1980). This term has a small but significant influence on the tidal behaviour (BLACK, 1983) over the entire harbour but it has a negligible influence over the smaller 2-dimensional model domain, where vertical stratification was also negligible. A no-flow (U = 0) condition was imposed at the upstream boundary while river inputs, which are small in Whangarei Harbour, were included in the appropriate cells.

The calibration and verification of the 1-dimensional model employed tidal water level and velocity comparisons. An example in Figure 3 shows that the model predicts the tidal water levels in the upper reaches (Figure 1) using the ocean water level as the input boundary condition at the seaward end. The bed friction coefficient (z_o) used in the model which gave this calibrated result was $z_0 = 0.0010$ m which compares favourably with the average roughness length of $z_o = 0.0007$ m obtained from velocity profile measurements throughout the lower harbour (BLACK and HEALY, 1982).

After calibration of the 1-dimensional model, the time series of mean sea levels at the 2-dimensional model boundary was extracted from the 1-dimensional simulation at the cross-section through One Tree and Reserve Points. The transverse variability about the mean sea level along this boundary, was determined by matching the model to the discharges in the two major channels measured with current meters. The 2-dimensional model was then given a detailed calibration (BLACK, 1983) using the 46 available time series of measured velocities (see later) as well as a series of drogue tracking experiments. An example of the resulting calibration is shown in Figure 4a,b. Notably, while the determination of mean level with the 1-dimensional model can be recommended as a useful general procedure, the method to find the transverse boundary gradients was applied only because computer memory limitations prevented the application of the more prudent procedure of moving the boundary away from the region of interest.

RESULTS

SEA BED DESCRIPTION

The sea bed investigations and side-scan sonar interpretation are summarized in the bed facies maps of Figure 5 and examples of bed types are shown in Figure 6. The percentage of sea bed covered by shell is large with the major channels being almost entirely floored by shell detritus. In the vicinity of the proposed marine terminal and the lower section of the Main Shipping Channel, the bed is distinguished by a compacted shell lag, often coated by algae coexisting with some sponge (Figure 6b), while in the entrance, the shell lag persists but it is clean and free of algal growth (Figure 6a). Upstream in the Main Shipping Channel, the bed is composed of cobble, shelly-gravel and biomass cover on the northern side changing to some loose sand and broken shell and then bedforms on the southern side (Figure 6c, d). A compacted lag occurs over much of the Shoal Bay Channel.

While stored sand is abundant on the banks and outside the entrance to the harbour, extensive sandy deposition is not evident in the major channels. This means that the sand has been and is continuing to be winnowed out leaving only the coarser, less-easily entrained shell and cobble sediments on the channel floors (BLACK and HEALY, 1982, 1983; MEHTA and CHRISTENSEN, 1983). Thus, where no sand is

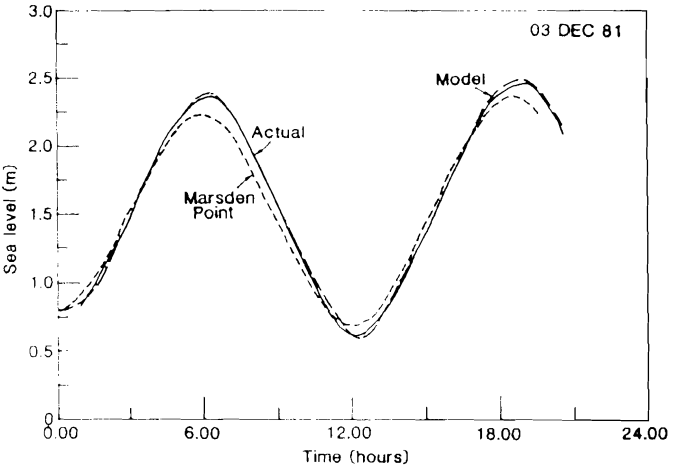

Figure 3. 1-dimensional model verification run for 3-DEC-81 with roughness length z_0 = 0.001 m compared to the actual tide levels at Whangarei Port located 16 km from the entrance.

available for entrainment, the local sandy bedload sediment transport in the channels is essentially zero. Moreover, a low suspended load transport is indicated where the lag is algae-encrusted because the fragile algae will not grow in a "sand-blasted" environment. The presence of pink coralline algal growths, which cannot flourish if the bed sediments are agitated so that they roll or rub together, similarly suggests that the lag sediments are also stable. Conversely, clean shell in the harbour entrance testifies to the passage of suspended sediment through the entrance throat or mobility of the shell detritus.

Bedforms

The major exceptions to the lagged channel floors are the bedforms lying along a distended ridge of sandy sediment linking Snake Bank with the south side of the entrance throat, the deposits of sand to the south-west of Darch Point and the distended ridge of sand on the south side of the lower section of the Shoal Bay Channel. Otherwise the major zones of active bedforms lie near the 5 m contour on the flanks of the channels; in particular on the south of the Main Shipping and Shoal Bay Channels.

Large, well-defined sand waves occur south of Darch Point in deposits of non-cohesive sands with minor fractions of broken shell. These bedforms, the biggest measured in the study area with wavelengths up to 50 m and heights of 1.6 m, disappear abruptly to their north off Darch Point where the bed returns to a stable algae-encrusted conglomeration of rock and shell (Figure 6b). These types of sudden transitions of the bed type are a feature of the region; sand/shell boundaries are abrupt enough for them to be observed by divers in some locations.

BATHYMETRIC STABILITY

The lower harbour was surveyed by the Royal New Zealand Navy in 1981. A previous survey had been undertaken in 1959/61 and Figure 7 shows the bed level changes that occurred over the 20 year interval. Sounding accuracy is limited to about 0.2 m in each survey so that the differences are expected to be insignificant unless they exceed at least 0.4 m. Moreover, errors in horizontal position fixing and sounding reductions may increase the error, particularly on the steep channel flanks where small horizontal deviations may result in vertical inaccuracies. Accordingly, only the changes exceeding 0.4 m are shaded in Figure 7 to show the regions where erosion/deposition may be significant.

The harbour is seen to be extremely stable with much of the region unchanged over the 20-year period. A notable example is the stability

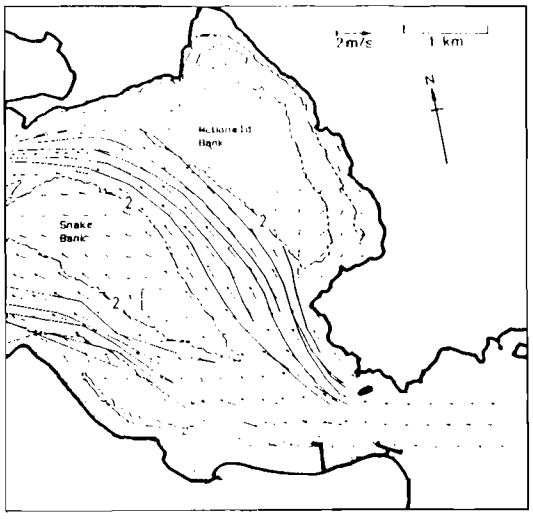

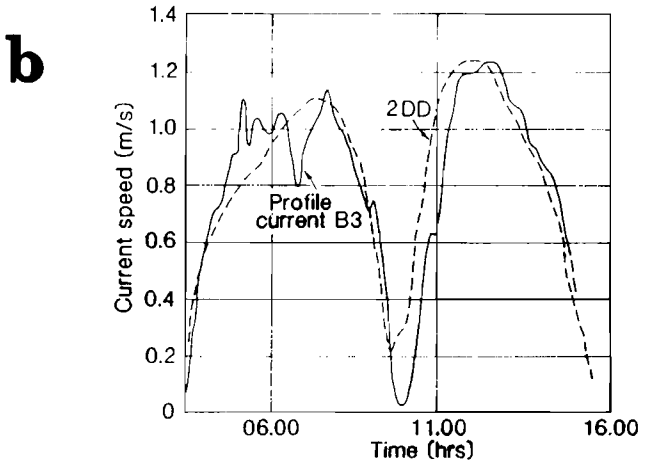

Figure 4a. Flood tide drogue paths in Whangarei harbour compared with the 2-dimensional model (2DD). The straight lines joining the drogue position fixes are not necessarily representing the actual flow path.
Figure 4b. Comparison of velocities measured in the entrance throat with the 2DD simulation for the calibration period 14-NOV-81.

in the entrance throat where depths have remained constant over large areas. In other locations, changes exceeding 0.4 m are patchy. The only area of significant change occurs to the north of One Tree Point and along the southern side of the Main Shipping Channel. In explanation, the Shell Cut Reach Channel, north of One Tree Point, was dredged by the Northland Harbour Board between bathymetric surveys. The large differences of -4.0 m and -2.2 m in Figure 7 show where the channel was taken through an existing sand bank to link with the Main Shipping channel, while the accretion to the south of Reserve Point is dredge spoil. The other changes to the north and south are apparently attributable to the alteration to the hydrodynamics after dredging. An important result of this comparison is the stability variation across the One Tree Point Channel. On the south side, where the bed is composed of a high percentage of sand, the erosion there reflects the expected increase in the currents arising after the dredged channel attracts higher flows into the Main Shipping Channel.

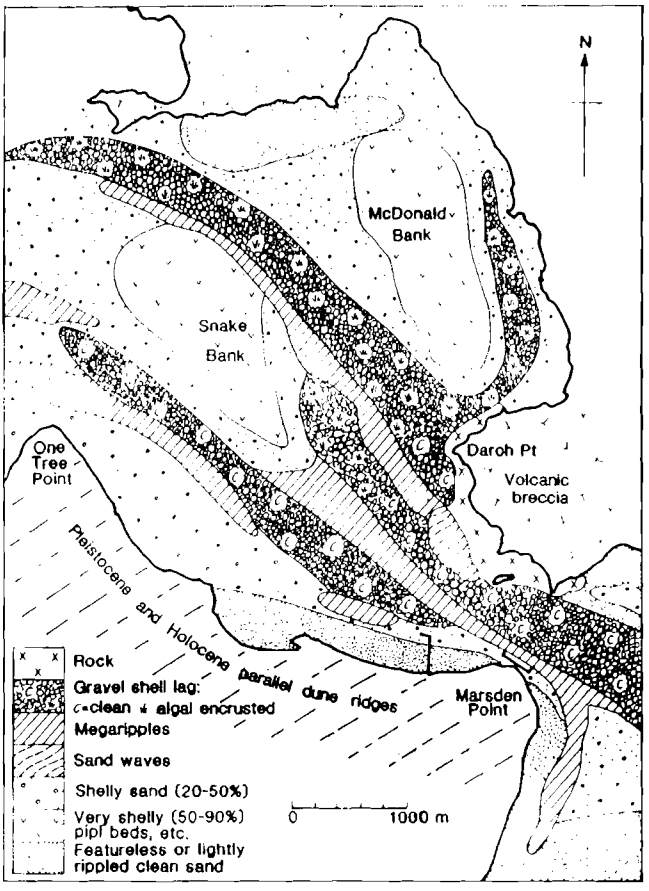

Figure 5. Simplified bottom sediment facies for Whangarei Harbour based on integration of side-scan sonar survey, underwater photographic and underwater video surveys, SCUBA diver observations, and bottom sediment analysis. The boundaries between facies are schematized.

However, although the tendency is for erosion, depth changes are less than 0.4 m and insignificant at the adjacent north side of the channel where shell content on the bed is higher. This is a clear indication that the general bed stability was enhanced by the shell lag sediments.

In summary, the comparisons of bathymetric surveys show the lower harbour to have been extremely stable excluding the effect of the channel dredging. This had already been inferred from the sea bed observations showing coarse, compacted, algal-encrusted shell lag over much of the harbour floor, implying a general bed stability and low suspended sediment load.

TIDAL FLOWS

Current meter site locations and the maximum measured speeds scaled to a spring tidal range of 2.2 m are shown in Figure 8. Currents are fast in the entrance channel and exceed 1 $m.s^{-1}$ during the spring tides. High flows are also evident in the two major channels and near Darch Point.

Sediment Threshold

The sandy sediment threshold speeds calculated using the method of BLACK and HEALY (1986) were compiled for three cases with the

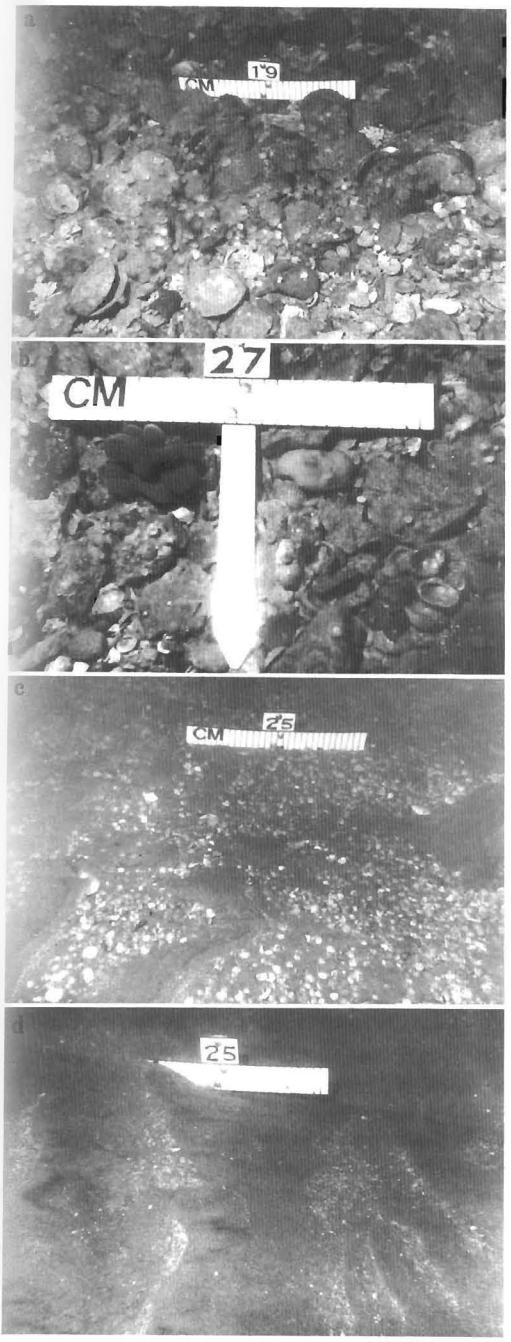

typical sand size of 0.3 mm (i) over a planar sand bed; (ii) over a planar shell bed; and (iii) over typical megaripple fields with heights of $h = 0.2$ m and wavelengths of $L = 4.0$ m. Over the megaripples the roughness length is found as,

$$z_0 = h^2 / 2L = 0.005 \text{ m} \quad (3)$$

Over the shell beds, the roughness is taken as

$$z_0 = k_s / 30.2 \quad (4)$$

Here k_s, the Nikuradse equivalent roughness, is approximately 0.01 m, reflecting the projection of the shells above the bed. Thus, $z_0 = 0.0003$ m.

This compares with a roughness length of 0.0002 m obtained by BLACK and HEALY (1982, their Table 1) using measurements of vertical velocity profiles above shell beds. Over planar sand beds, BLACK and HEALY (1986) suggested a roughness length of $z_0 = 0.0001$ m. With these roughness lengths, the threshold velocities at 1 m above the bed determined using Table 2 in BLACK and HEALY (1986) are presented here in Table 1.

As is indicated by the presence of megaripples in the harbour (Figure 5), the velocity measurements (Figure 8) consistently exceed the sediment threshold speed of 0.29 $m.s^{-1}$ over the sandy beds. The currents in the channels over the shell lagged beds also exceed the threshold speed of about 0.45 $m.s^{-1}$. Thus, the flows have the capacity to move sandy sediments around most of the lower harbour and the stability of the region is not simply due to incompetent currents.

Shell Thresholds

Several experiments to find in situ shell thresholds in Whangarei Harbour are reported by BLACK (1983). In each of these experiments, no movement of the shell bed was seen even though shells were observed in currents up to 0.9 $m.s^{-1}$ at 1 m above the bed. This observation concurs with the series of measurements by MEHTA and CHRISTENSEN (1983) on the

Figure 6 (a-d) (Adjacent column). The nature of the bed in Whangarei Harbour: (a) Gravel shell lag from the entrance gorge comprised mainly of the Dog Cockle (*Glycymeris laticostata*) and scallop (*Pecten nouvouzelandae*). (b) Algal and sponge growths on gravel rock and shell lag off Darch Point. (c and d) Sandy ripples on megaripples and shelly sand off the southeastern tip of Snake Bank. Large variation over small distances was common in Whangarei Harbour.

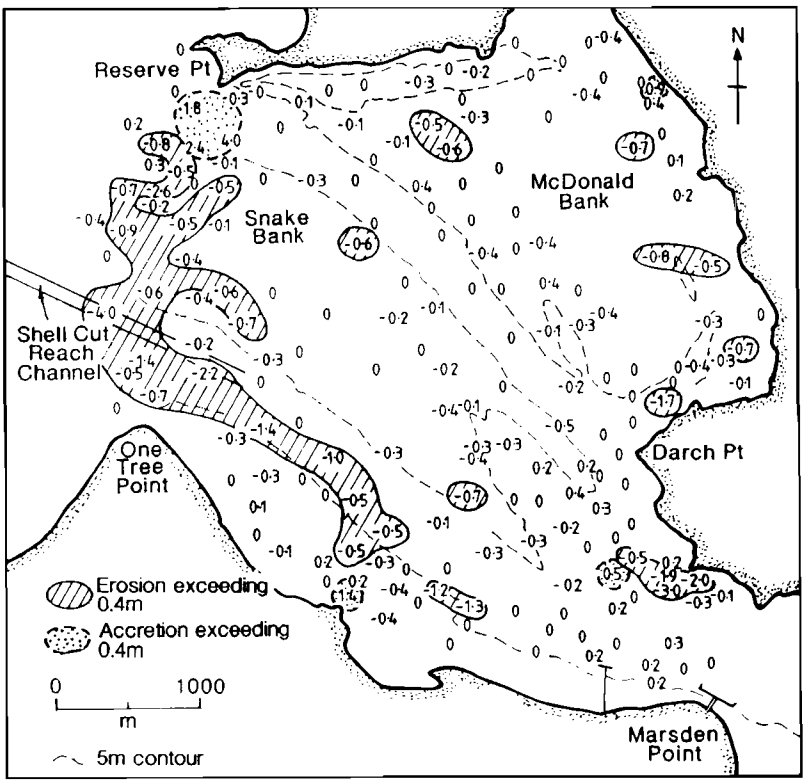

Figure 7. Lower Whangarei Harbour showing comparison of 1959/1961 and 1981 hydrographic surveys undertaken by the Royal New Zealand Navy, Hydrographic Branch. Depth changes in metres.

Florida coast. In Whangarei Harbour, currents were never fast enough to move the shells even though both SCUBA and underwater video observations were made during periods of spring tides.

MEHTA *et al.* (1980) measured the fall velocity of disarticulated common bivalve shells and, for the cockle (*Chione stutchburyi*) which is common in Whangarei Harbour, they report a mean fall velocity of 0.24 $m.s^{-1}$. BLACK (1984) confirmed this result by measuring fall velocities of several common shell types from Tauranga Harbour, another tidal estuary on the east coast of New Zealand's North Island. This high fall velocity compares with 0.032 $m.s^{-1}$ for 0.3 mm quartz sand (RAUDKIVI, 1976). Over a planar bed, the Yalin threshold curve (*e.g.* MILLER *et al.*, 1977) predicts a critical friction velocity (u_*) of 0.059 $m.s^{-1}$ for a density of 2790 $kg.m^{-3}$ and a shell size of 5 mm. Applying this in the Karman Prandtl logarithmic vertical velocity profile equation with $z_0 = 0.0003$ m, one obtains for the critical erosion velocity at 1 m above the bed,

$$u_{1cr} = 5.75\ u_* \log_{10}(1/z_0) = 1.18\ m.s^{-1} \quad (5)$$

This very high velocity exceeds most of the measurements in Whangarei Harbour. Moreover, the threshold speed may increase for larger shells (50–60 mm shells are common) or if the shells have been imbricated by mechanical current action or bound together by biological action. Contrary to this, the shells have a large surface area and are subjected to a higher form drag in proportion to their weight than a sand grain. This may temporarily reduce the threshold speed making them unstable until they rest with an orientation that reduces the form drag to below threshold levels. Experiments in Whangarei Harbour showed that loose shells, when dropped to the sea bed in fast current flows, initially rolled or vibrated, but typ-

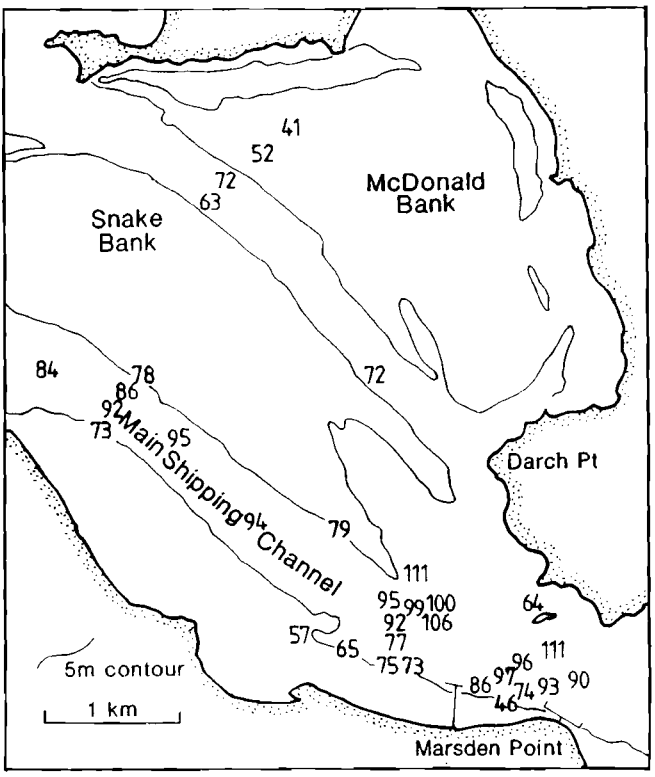

Figure 8. Maximum measured current speeds (cm.s^{-1}) at peak tidal flow scaled to a common spring tide range of 2.2 m.

Table 1. *Sediment threshold speeds over three types of bed for a sandy grain size of 0.3 mm and quartz density of 2650 kg. m^{-3}*

Bed type	Roughness length (m)	Threshold speed (m.s^{-1})
planar sand bed	0.0001	0.46
planar shell bed	0.0003	0.43
rippled sand bed	0.005	0.29

ically found low form drag orientations within seconds of their impact with the bottom, and observable movement ceased (BLACK, 1983).

While there may be some error in the estimate of the shell threshold speed, it is clear that the shell lagged beds are highly stable as demonstrated by the field experiments and the calculation of the threshold velocity. With biological action to bind the bed sediments, the measurements confirm that the algae-encrusted shell lags which commonly occur in the channels are likely to be completely stable.

Thus, the long-term stability of the harbour is seen to occur in a bed facies environment dominated by the presence of the shell lags on the channel floors. Juxtaposed within this environment are the sudden transitions to pockets or distended "pathways" of sandy sediment, often lying adjacent to overgrown and stable lag beds (Figure 6b). The following sections of this paper examine the mechanism that makes this possible, isolating the flow characteristics that determine local bed type.

IMPLICATIONS FOR NET SEDIMENT TRANSPORT AROUND SNAKE BANK

The bedforms extending from Snake Bank to the entrance are distinguished by a notable variation in their character across the ridge. The bedforms on the south side are reversing megaripples with typical wavelengths of 3–5 m and heights of 0.15–0.20 m. A short distance to the north, an abrupt and marked increase in

their wavelength occurs (putting them into the sand wave category) and they develop an up-harbour or flood orientation. These northern sand waves persist into the shallow inter-tidal zones on the face of Snake Bank as seen in the aerial photograph of Figure 2.

The presence of the sand waves on the northern side of the sediment ridge is indicative of an asymmetrical tidal flow (BOOTHROYD, 1978, modified after HARMS *et al.*, 1975), which is flood-directed in this case. Confirming this, the morphology of the area is that of a flood ramp (HAYES and KANA, 1976) to the Snake Bank delta which receives the decelerating flood currents from the entrance gorge. The flood ramp is bounded by a second ridge of sandy sediment along the adjacent Shoal Bay Channel, while the bed between these two ridges of loose sand is predominantly an algae-coated shell lag.

With flood dominance on the flood ramp, the bounding ridges of sand are expected therefore to lie in zones where currents are more neutral between the flood ramp and adjacent ebb dominant flows. In this case, Snake Bank follows closely the HAYES and KANA (1976) model of a typical flood-tidal delta with identifiable features of ebb shield, ebb spit, flood ramp and flood channel. The ebb spit lies between the flood dominated flood ramp and the ebb dominated flow in the channel.

Shallow water currents recorded at several locations around Snake Bank (Figure 9) are consistent with the implications from the bedforms and morphology. Flood dominance occurs at the north-east of the flood ramp and continues along the north-east side of Snake Bank. Ebb dominance occurs adjacent to the shipping channel. Thus, the supportive evidence suggests that the net circulation of sediment around Snake Bank is depicted by the directions shown in Figure 9.

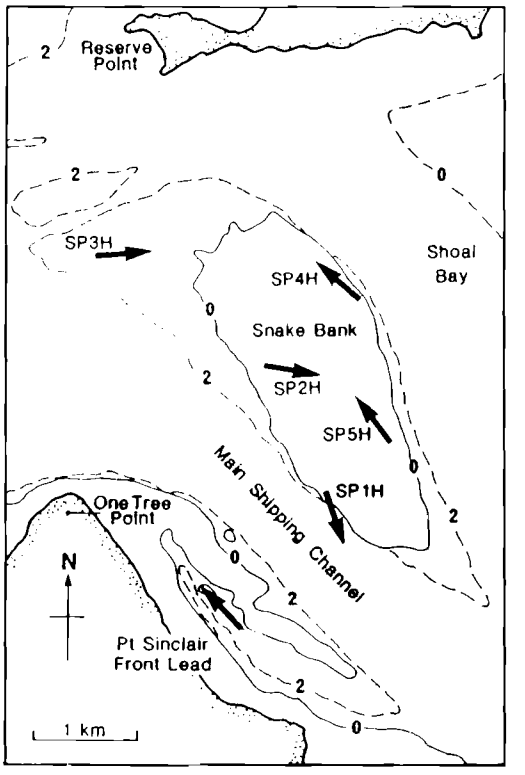

Figure 9. Snake Bank flood-tidal delta and the inter-tidal zone up to One Tree Point showing current meter measurement sites and the current direction at peak flow during the tidal cycle.

The Shell Ridge

Snake Bank is subjected to a net flood flow on the entrance side of the snake-like shell ridge and net ebb flow to its north (Figure 9). As confirmed by the orientation of sand waves in the aerial photograph of Figure 2, the snake-like shell ridge separates the ebb and flood dominant zones and is therefore sub-aerial deposition in a zone between opposed net currents. In terms of the gross morphology, the entrance end of Snake Bank is a flood-tidal delta relative to the entrance throat, while the up-harbour end is partly an ebb shield and partly an ebb-tidal delta relative to the constricted cross-section between One Tree and Reserve Points, with the shell ridge separating the two hydrodynamic environments.

RESIDUAL CURRENT VELOCITIES

To determine the net flow directions throughout the harbour, residual velocities and distances were determined for all current meter sites (Figure 10) after scaling to a constant tidal range. The residual velocity was defined as the net current over one complete tidal cycle obtained by vector averaging the measured velocities which exceeded a selected threshold.

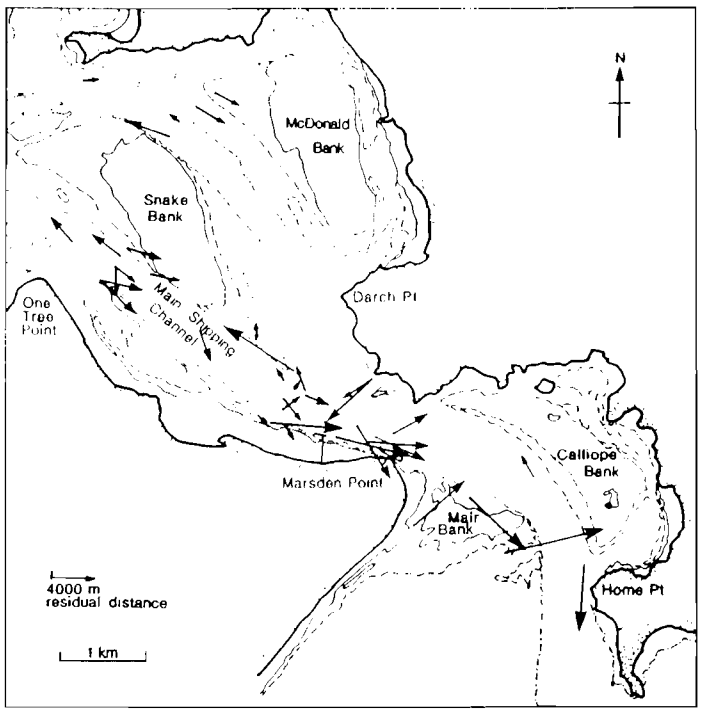

Figure 10. Measured tidal cycle residual distances at 1 m above the sea bed for periods when the speed exceeded 0.33 $m.s^{-1}$.

The residual distance was this velocity multiplied by the time that the currents exceeded the threshold. With a zero threshold speed, the time multiplier is constant (12 hrs 25 mins in semidiurnal tides) and the residual distance and velocity are equivalent. However, for other thresholds, the residual distance gives an indication of current asymmetry above threshold as well as the period that this asymmetry acts and is accordingly a better indicator of net bedload sand transport. To depict net sediment circulation, residual distances were calculated with a threshold speed everywhere of $u_t = 0.33$ $m.s^{-1}$, an average threshold for Whangarei sands (Table 1). Both the profile measurements and the velocities provided by the hydrodynamic model were employed.

Profile Measurements

Figure 10 shows that the measured flows have a strong ebb dominance at the south side of the entrance with ebb dominance continuing up the Main Shipping Channel as far as One Tree Point. The large flood-directed vector on the flood ramp confirms previous results. To the immediate south of this on the sediment ridge, currents pass from flood dominated through neutral to become ebb dominated. This again is consistent with previous deductions from the morphological and bedform analyses around Snake Bank. In the Shoal Bay Channel, currents are flood dominated next to Snake Bank and turn net ebb around the face of McDonald Bank. The flood vector next to Snake Bank is a continuation into the channel of the flood dominance measured on the bank in shallow water (Figure 9).

HYDRODYNAMIC MODEL RESULTS

On its regular grid, the numerical model's comprehensive spatial representation of the flows provides the detail necessary to specify the relationship of current flow to bed type throughout the lower harbour. The model, 2DD,

was applied in Whangarei Harbour to several applications, but for this paper, the most relevant of these is the determination of sediment transport patterns as depicted by the residual distances. As already noted. The model has been calibrated using all of the velocity measurements in the harbour (BLACK, 1983), so the correspondence to be seen between the measured and model predicted residual distances is to be expected.

Calibrated model flow patterns at 2-hourly intervals during the tidal cycle are shown in Figure 11. The major features evident in the model simulation are the large inter-tidal deltas and harbour margins which flood and dry during the tidal cycle. The fastest currents pass along the Shoal Bay and Main Shipping Channels while McLeod Bay receives only low flows. Strong currents occur at the entrance and Marsden Point, and where the flow streamlines converge at Darch Point. The shell ridge on Snake Bank turns the ebb currents to the north around the obstruction.

Residual distances were calculated in each cell by accumulating modelled velocities above the mean vertically-averaged velocity threshold of $U = 0.40\ m.s^{-1}$ at 1 minute intervals over the tidal cycle (Figure 12, *cf* profile measurements in Figure 10). Patterns of net circulation predicted by the model are summarized in Figure 13.

Clearly, there is potential for sediment to travel around closed loops within this region in conjunction with a throughput at the entrance and the One Tree Point boundaries. For example, the net flood currents on the flood ramp continue north-west to create an unbroken "sediment pathway" to the north of Snake Bank, with return transport in the Shoal Bay Channel reuniting with the flood ramp, up-harbour residual to the south of Darch Point. This potential for local recirculation within a region implies that interference with a closed loop can be expected to have an influence around all of the loop. The size of the loop shown by the 2-dimensional model demonstrates the scale of the potential for interaction between different regions in an estuary. In Whangarei Harbour, while the flood ramp is seen to be directly connected to the Shoal Bay Channel and the north of Snake Bank, the Main Shipping Channel is primarily a one-way transport pathway directed out of the harbour.

MORPHOLOGICAL AND EROSION/ DEPOSITION IMPLICATIONS

While numerical sediment transport modelling was undertaken in Whangarei Harbour, the processes responsible for the variable bed types are better understood in terms of the current residuals. In 1-dimension, consider a sandy bed divided longitudinally into equal compartments with varying current intensities and residual distances in each. For simplicity we assume that the residual distance is a linearly proportional measure of the bedload sediment transport capacity. Sediment transport rates have been shown to be proportional to the cube of the velocity excess above threshold (GADD *et al.*, 1976; BLACK and HEALY, 1982) but the residual distance, defined using the cube of the velocity excess, gave results mostly similar to the linear case (BLACK, 1983) and the linear assumption is adequate for this discussion.

Scour will occur in a compartment if its residual is greater than the one upstream and deposition results from the opposite condition. In general terms, net loss conditions are reflected by increasing residuals in the (net) downstream direction and vice versa. This is essentially a restatement in terms of the residual distance of a commonly accepted understanding of the mass conservation equation over sandy beds in steady flows. The residual distance is introduced to account for flow unsteadiness and substitutes for the flow velocity.

In this context, the presence of shell lags is expected to reflect erosive conditions, *i.e.* sand cannot settle because the potential for output from the region, as indicated by the residual distances, is greater than the input. Conversely, sandy beds should occur where the residual distances are at least neutral or decreasing in the downstream direction. It should be noted that this result does not depend on absolute current speed above the sandy sediment threshold.

A second important factor, which only arises over lagged beds, is the "availability" of sandy sediment (BLACK, 1983, 1984, 1987). If only limited inputs are available, such that the current has the potential to carry much larger quantities, then the residual distance will no longer be in proportion to the actual sediment transport rates. Returning to the 1-dimensional condition, deposition can only occur in the first

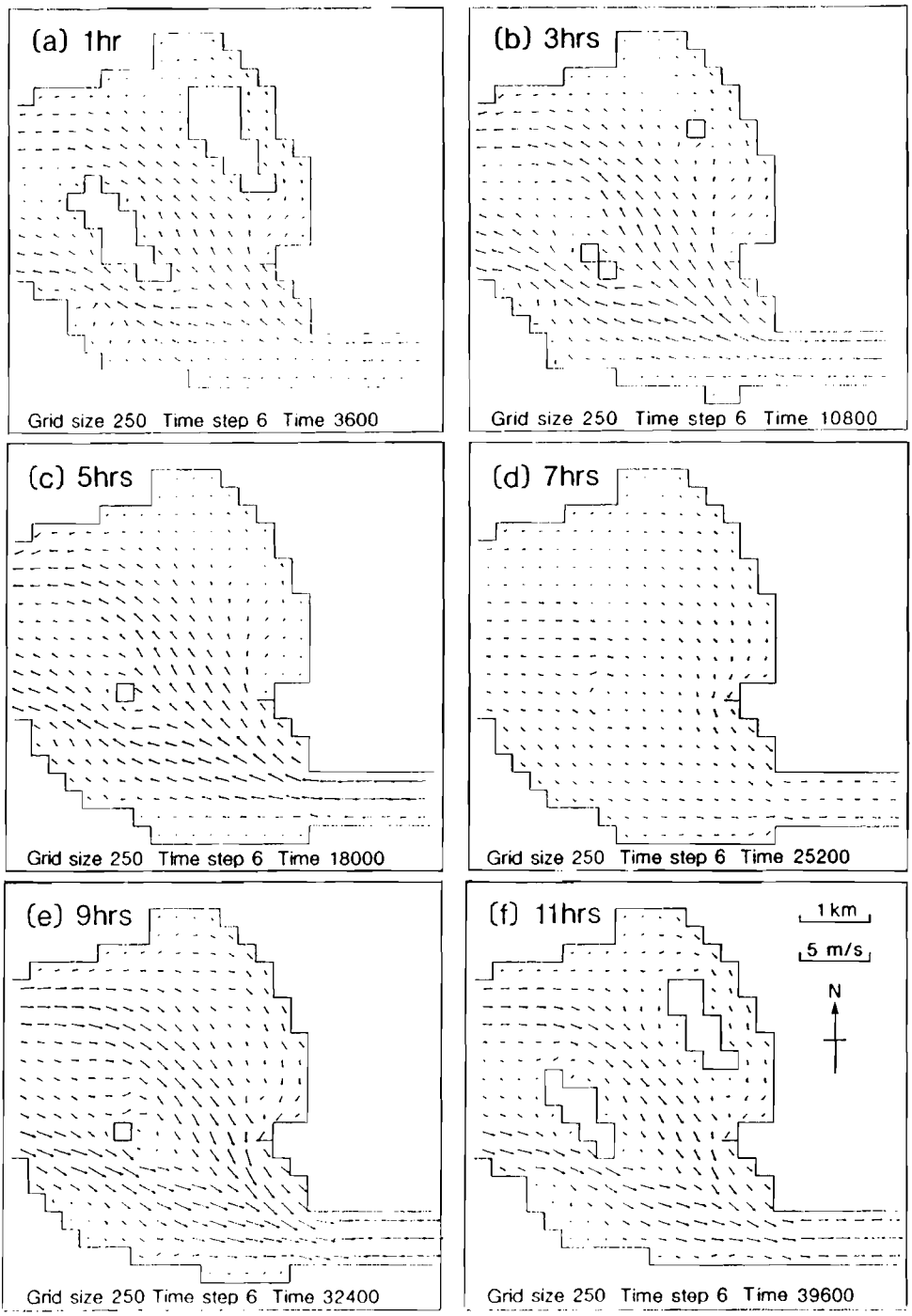

Figure 11 (a-f). Numerical simulation of flow patterns in Whangarei Harbour at various stages of the tidal cycle (hours after low water for the spring tide of 14-DEC-81).

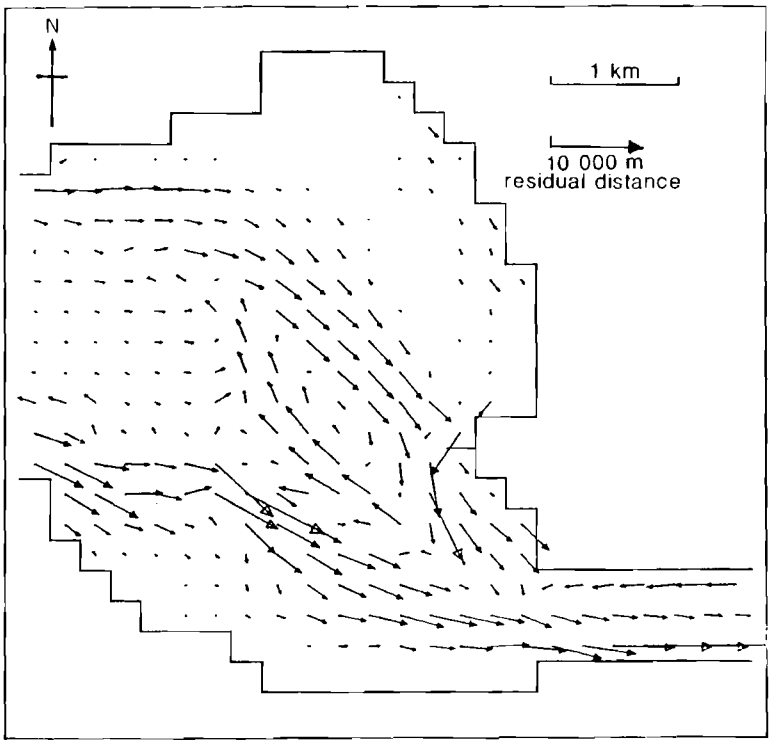

Figure 12. Model tidal cycle residual distances for velocities exceeding 0.4 $m.s^{-1}$ for a spring tidal simulation on 14-DEC-81 with ebb and flood velocities scaled to a common tidal range of 2.6 m.

"cell" where the material entering from upstream exceeds the amount that the local cell can remove. Otherwise, deposition will not occur, even if the residual distances decrease downstream.

Whangarei Harbour

When the nature of the bed is assessed in terms of the local variation in residual distance (Figure 12), the occurrence of localized shell and sand beds can be explained with the above interpretation. The Main Shipping Channel is subjected to a strong net ebb residual which increases downstream near the entrance and shell lags result. The bedforms on the channel flank near One Tree Point occur where the residual diminishes rapidly, changing from ebb to flood dominated. Similarly, the bedforms north of One Tree Point occur in the neutral zone between the ebb and flood dominant flows. The sediment ridge extending towards the entrance from Snake Bank corresponds precisely with the region of neutral net flow predicted by the model. The lagged bed on the flood ramp corresponds with the increasing flood residuals there. The bedforms in Shoal Bay to the north-east of Snake Bank occur where the flood residual is diminishing and the continuation of this to the south corresponds with the neutral zone along the south side of Shoal Bay Channel. The Shoal Bay Channel is subjected to net ebb residuals which increase downstream and is lagged. The large bedforms south of Darch Point occur where the ebb residual rapidly decelerates there. Thus, there is correspondence without exception to this principle throughout the lower harbour where tidal currents are above the medium sand threshold. Figure 12 shows currents are rarely above threshold in the McLeod Bay channel and this is in accordance with the occurrence of finer sediments there.

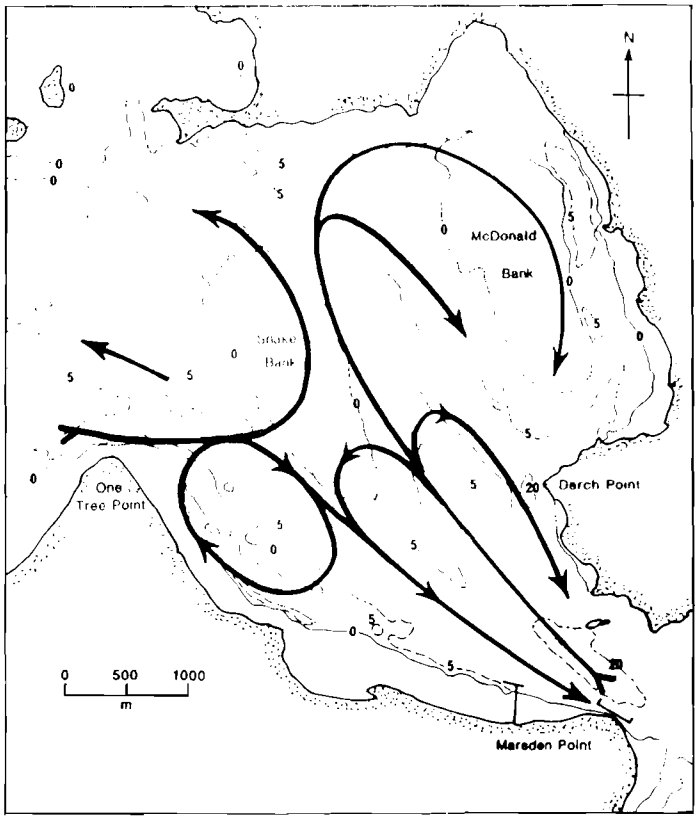

Figure 13. Schematic diagram showing sediment transport loops and pathways revealed by the residual velocities and distances from the 2 dimensional model taken in conjunction with field observations and measurements.

IMPLICATIONS FOR THE MARINE TERMINAL SITE

The proposed marine terminal (Figure 1) is sited on Marsden Point at the southern end of the Main Shipping Channel and the dredged basin is seen to extend from Marsden Point across the channel and onto the ebb spit extending from Snake Bank. The existing 8-m deep channel margin platform in the Main Shipping Channel is to be dredged to 13 m below chart datum.

In view of the above results, the southern end of the dredged basin (where the shell lag presently exists) will be subject to deposition only if the currents are reduced to a level where the sediment inputs from the channel exceed the carrying capacity of the flows after construction. The net ebb imbalance is presently distinctive in this region and the above analyses strongly suggest that deposition therefore should be minimal. It is noted too that the design includes reclamation designed to maintain the present channel cross-sectional area after dredging, and thus keep average current changes in the cross-section to a miniumum.

The northern edge of the dredged basin dissects the ebb spit from Snake Bank. In view of the capacity for sediment transport identified there, it would be expected that some sediment will deposit in the north-west corner. Because of the alteration to the hydrodynamics caused by construction, it is not possible to accurately determine the deposition quantities with existing measurements. Numerical sediment transport modelling was required (BLACK, 1983) and while this is not under discussion here, it was found that sedimentation in the dredged

basin should lie in the range of 10,000-30,000 $m^3.yr^{-1}$. This result reflects the stability and low net sediment transport rates identified in Whangarei Harbour and is much less than one would expect for a sandy harbour subjected to currents of about 0.8 $m.s^{-1}$. For example, a current of this strength will transport approximately 0.07 $kg.m^{-1}.s^{-1}$ of sand (BLACK and HEALY, 1983). Over a dredged basin of 450 m width and if the current acts for about 8 hours per tidal cycle, this converts to an upper limit of 230,000 $m^3.yr^{-1}$, assuming all material entering the dredged basin remains there.

CONCLUSIONS

Several experimental procedures were utilised to describe the nature of the bed and specify the sediment dynamics of the lower section of a large estuary. Much of the bed is floored by a shell detritus, particularly in the major channels. Algae coating and the presence of the shells indicate low sediment transport rates and a stable bed. Comparisons of bathymetric surveys revealed that the lower harbour is very stable with essentially no change to bathymetry in many areas over a 20-year interval. Recorded tidal flows were found to be faster than the threshold speed for typical sandy sediments, but not competent to disturb lagged shell beds. This concurred with the bathymetric comparisons showing a stable harbour. Examination of the morphology of the Snake Bank flood-tidal delta indicated that bedform interpretation, gross morphology implications and direct current measurements provided a consistent description of circulation around the bank. This was extended to include other measurements, especially interpretation from residual velocity distances and, with results from a numerical hydrodynamic model, the sediment circulation patterns in lower Whangarei Harbour were described. Using the model results, the location of shell and sand beds was explained in terms of spatial changes to sediment transport capacity and the availability of sandy sediments. The suitability of a proposed marine terminal site was interpreted using these results.

ACKNOWLEDGEMENTS

The authors would like to thank the Northland Harbour Board which funded this project and provided assistance with the field measurements. Colin Squires, Warren King and Mike Beazley assisted with many aspects of the study. The Royal New Zealand Navy Hydrographic Branch and Diving Tender made many useful contributions. Use of University Grants Committee equipment is acknowledged. Margaret Sweeney and Annette Field typed the manuscript, and Frank Bailey draughted the diagrams.

LITERATURE CITED

BIORESEARCHES LTD, 1976. *Aspects of the ecology of the areas surrounding the oil refinery at Marsden Point*, a report to the New Zealand Refining Company, Marsden Point. 190p.

BLACK, K. P., 1983. *Sediment transport and tidal inlet hydraulics*. D. Phil. Thesis, University of Waikato, Hamilton, New Zealand, Vol. 1 (text 331 p.) and Vol. 2 (figures).

BLACK, K. P., 1984. *Sediment transport. Tauranga Harbour Bridge*. A Report to the Bay of Plenty Harbour Board, Mount Maunganui, New Zealand. Vol. 1 (text, 159 p.) and Vol. 2 (figures).

BLACK, K. P., 1987. A numerical sediment transport model for application to natural estuaries, harbours and rivers. In: J. NOYE, (ed.), *Numerical modelling: applications to marine systems*. Amsterdam: North Holland Mathematics Studies. Elssevier, pp. 77–105.

BLACK, K. P. and GAY, S. L., 1987. Eddy formation in unsteady flows. *Journal of Geophysical Research*, 92(C9), 9514-9522.

BLACK, K. P. and HEALY, T. R., 1982. Sediment transport investigations in a New Zealand tidal inlet. *Proceedings of the 18th International Engineering Conference* (American Society of Civil Engineers), pp. 2436–2457.

BLACK, K. P. and HEALY, T. R., 1983. *Side-Scan Sonar Survey*. Marsden Point Forestry Port Investigations. Northland Harbour Board. Whangarei, New Zealand, 88 pp.

BLACK, K. P. and HEALY, T. R., 1986. The sediment threshold over tidally-induced megaripples. *Marine Geology*, 69, 219–234.

BLACK, K. P.; HEALY, T. R., VENUS, G., STOAKES, J. and HUNTER, M., 1981. *Sea Floor Photographic Survey*. Marsden Point Forestry Port Investigations. Northland Harbour Board, Whangarei, New Zealand, 149p.

BLACK, K. P.; BEAZLEY, M. J. and HUNTER, M., 1982. *Channel drogue tracking*. Marsden Point Forestry Port Investigation. Northland Harbour Board, Whangarei, New Zealand, 73p.

BOOTHROYD, J. C., 1978. Tidal Inlets and Tidal Deltas. Chapter 7 in R. A. Davis, (ed.), *Coastal sedimentary environments* (2nd ed.). New York: Springer-Verlag, pp. 445–532.

DANISH HYDRAULICS INSTITUTE, 1982. *Proposed Forestry Terminal. Hydraulic Model Studies*. Report

to the Northland Harbour Board, Whangarei, New Zealand, 132p.

GADD, P. E.; LAVELLE, J. W. and SWIFT, D. J. P. 1978. Estimates of sand transport on the New York shelf using near-bottom current-meter observations. *Journal of Sedimentary Petrology*, 48, 239–252.

HARMS, J. C.; SOUTHARD, J. B., SPEARING, D. R. and WALKER, R. G. 1975. *Depositional environments as interpreted from primary sedimentary structures and stratification sequences.* Lecture Notes, SEPM Short Course No. 2. Dallas, Texas. 161p.

HAYES, M. P. and KANA, T. W., 1976. *Terrigenous clastic depositional environments.* Technical Report No. 11-CRD, Department of Geology, University of South Carolina, 302p.

HEALY, T. R., 1981a. Assessment of the Sedimentological, Hydrological and Biological Impacts of the Proposed Off-loading Ramp at Marsden Point. *Part A: Sedimentation Aspects, Bioresearches Ltd Report* to the New Zealand Refining Company, Marsden Point. 1–48.

HEALY, T. R., 1981b. Sediments and Hydraulics in the Vicinity of the Proposed Timber Port at Marsden Point. *Northland Forestry Port Marsden Point Environmental Impact Report Supplementary Appendices.* pp. 1–51.

HEALY, T. R.; BLACK, K. P. and DE LANGE, W. P., 1987. Field investigations required for numerical model studies of port developments in large tidal inlet harbours. *International Geomorphology*, 1, 1099–1112.

LEENDERTSE, J. J., 1967. Aspects of a computational model for long-period water-wave propogation. *Research Memorandum RM-5294-PR, Rand Corporation*, Santa Monica, California.

MEHTA, A. J. and CHRISTENSEN, B. A., 1983. Initiation of sand transport over coarse beds in tidal entrances. *Coastal Engineering*, 7, 61–75.

MEHTA, A. J.; LEE, J. and CHRISTENSEN, B. A., 1980. Fall velocity of shells as coastal sediment. *Journal of the Hydraulics Divison (American Society of Civil Engineers).* HY 11 1727–1744.

MILLAR, A. S., 1980. *Hydrology and surficial sediments of Whangarei Harbour.* M.Sc. Thesis, University of Waikato, Hamilton, New Zealand, 212p.

MILLER, M. C.; McCAVE, I. N. and KOMAR, P. D., 1977. Threshold of sediment motion under unidirectional currents. *Sedimentology*, 24, 507–527.

RAUDKIVI, A. J., 1976. *Loose boundary hydraulics.* New York: Permagon, 397p.

[ ] RÉSUMÉ [ ]

Plusieurs campagnes de terrain et un modèle numérique hydrodynamique ont permis de déterminer les caractéristiques du transport sédimentaire dans la section inférieure d'un large estuaire à dominante tidale: Whangarei Harbour au NW de la Nouvelle Zélande. Dans ce cas inhabituel où les traînées de coquilles et les mélanges sables coquilles ont une influence dominante sur le transport sédimentaire net, les résultats soulignent un réseau cohérent, même si l'estuaire est soumis à une large gamme de flux dont la compétence est largement au dessus du seuil de mise en mouvement du sédiment. Décrit la capacité de transport sédimentaire dans l'estuaire. Présente et discute l'influence des lits de traînée, les relations morphologie, sédiments, dynamique tidale, particulièrement la vitesse résiduelle des courants de marée, et ce que cela implique pour l'implantation d'un terminal marin dans la zone étudiée.—*Catherine Bressolier, E.P.H.E., Montrouge, France.*

[ ] RESUMEN [ ]

Se ha aplicado una serie de investigaciones de campo y un modelo numérico hidrodinámico para determinar las caracteristicas del transporte de sedimentos en la sección inferior de un gran estuario mareal en Whangarei Harbour, en el nordeste de Nueva Zelanda. El resultado muestra un patrón estable en este caso inusual en el que las mezclas de arenas conchiferas y cementadas tienen una influencia dominante en el transporte neto de sedimentos aunque el estuario esté sujeto a flujo bien por encima del umbral de movimiento. Se presenta y analiza una descripción de la capacidad de transporte de sedimento del estuario, la influencia de los lechos cementados, la relación entre la morfologia y sedimentos y la dinámica mareal, especialmente las velocidades residuales de los ciclos de marea y las implicaciones para una terminal marina propuesta en la región de estudio.—*Department of Water Sciences, University of Santander, Cantabria, Spain.*

[ ] Zusammenfassung [ ]

Eine Reihe von Feldforschungen und ein numerisches hydrodynamisches Modell wurden angewandt, um die Merkmale des Sedimenttransports im unteren Abschnitt eines großen, durch die Gezeiten beherrschten Ästuars bei Whangarei Harbour, Nordost-Neuseeland, zu bestimmen. Die Resultate zeigen ein konsistentes Muster für diesen ungewöhnlichen Fall, wo Muschelreste und Muschel-Sand-Gemische einen vorherrschenden Einfluß auf den Netto-Sedimenttransport haben, obwohl der Ästuar einem breiten Spektrum bedeutender Strömungen unterworfen ist, deren Geschwindigkeit über der für sandiges Sediment notwendigen Schwelle liegen. Vorgestellt und diskutiert werden eine Beschreibung der Kapazität des Ästuars in Bezug auf Sedimenttransport, der Einfluß von residualen Sedimentbänken, die Beziehung von Morphologie und Sedimenten zur Gezeitendynamik und die Folgerungen für den beabsichtigten Bau eines Hafens.—*Helmut Brückner, Geographisches Institut, Universität Düsseldorf, F.R.G.*